

# Persistent unstable atmospheric boundary layer enhances sensible and latent heat loss in a tropical great lake: Lake Tanganyika

Piet Verburg<sup>1,2</sup> and Jason P. Antenucci<sup>3</sup>

Received 17 July 2009; revised 17 January 2010; accepted 22 January 2010; published 8 June 2010.

[1] Energy fluxes across the surface of lakes regulate heat storage and affect the water balance. Sensible and latent heat fluxes are affected by atmospheric stability, especially for large lakes. We examined the effect of atmospheric stability on the heat fluxes on seasonal time scales at Lake Tanganyika, East Africa, by estimating hourly sensible and latent heat fluxes and net radiation using thermistor chains and meteorological stations. The atmosphere was almost always unstable, in contrast to the atmosphere above North American Great Lakes which is unstable in winter and stable in summer. Persistent atmospheric instability resulted in a 13% and 18% increase in the annual mean heat loss by latent and sensible heat fluxes, respectively, relative to conditions of neutral stability. The persistent unstable atmosphere is caused by a higher water surface temperature compared with air temperature, which we argue is the case in general in (sub)tropical lakes. Low humidity further enhanced the frequency of unstable conditions and enhanced the exchange of heat and vapor from the lake to the atmosphere. The estimated heat fluxes were sensitive to the temporal scale of data inputs and to the local values of parameters such as air density. To our knowledge this is the first paper that demonstrates and quantifies the effect of atmospheric stability on latent and sensible heat fluxes from a lake on an annual basis, using data collected from the lake surface.

**Citation:** Verburg, P., and J. P. Antenucci (2010), Persistent unstable atmospheric boundary layer enhances sensible and latent heat loss in a tropical great lake: Lake Tanganyika, *J. Geophys. Res.*, 115, D11109, doi:10.1029/2009JD012839.

## 1. Introduction

[2] The heat budget for a lake is the most fundamental component of physical limnology, and is controlled by interaction with the atmosphere. These interactions are affected by the stability of the atmospheric boundary layer above the surface of the lake. The atmosphere above the surface of a lake is unstable and convective when the Obukhov stability length is negative [Brutsaert, 1982]. The difference between the air and water-surface temperature can be used as an indicator of stability [Derecki, 1981; Croley, 1989] with an unstable atmosphere typically associated with a water surface temperature that exceeds the air temperature, although this is not strictly correct as wind speed and humidity also need to be considered.

[3] Heat loss from a lake by sensible heat and latent heat transfer is enhanced when the atmosphere above it is unstable and reduced when the atmosphere is stable [Brutsaert, 1982]. Unstable atmospheric conditions over lakes can persist for long periods [Rouse *et al.*, 2003]. Lakes, as opposed to the

ocean, generally experience more extreme variability in atmospheric boundary layer stratification (i.e., from highly stable to highly unstable) due to the greater heating and cooling by the surrounding land and also due to the generally lower wind speeds [Katsaros, 1998].

[4] To examine the effect of atmospheric stability on latent and sensible heat fluxes during a full year in a tropical lake, heat fluxes across the water surface of Lake Tanganyika were determined using aerodynamic methods. Latent and sensible heat fluxes were estimated on an hourly basis from wind speed, air temperature, surface water temperature, humidity, and air pressure (as detailed below).

[5] In the method section we give special attention to variables, components of the algorithm used to compute energy fluxes, which are adjusted for high tropical temperatures and altitude above sea level (low air pressure). We examined to what extent the local, tropical values of latent heat of vaporization, air density and viscosity of air affect the heat fluxes and the stability effect. The discussion below places the results in the context of previous work on the Laurentian Great Lakes and argues that persistent unstable boundary layers are probably common in tropical lakes.

## 2. Study Area

[6] Lake Tanganyika is a deep Rift Valley lake in East Africa (maximum depth 1470 m, Figure 1), the second largest by area in Africa ( $32,600 \text{ km}^2$ ) and second deepest lake in the world. It is located between  $3^\circ$  and  $9^\circ \text{ S}$ , is 670 km long and

<sup>1</sup>National Center for Ecological Analysis and Synthesis, Santa Barbara, California, USA.

<sup>2</sup>Now at Aquatic Ecology, National Institute of Water and Atmospheric Research, Hamilton, New Zealand.

<sup>3</sup>Centre for Water Research, University of Western Australia, Crawley, Western Australia, Australia.

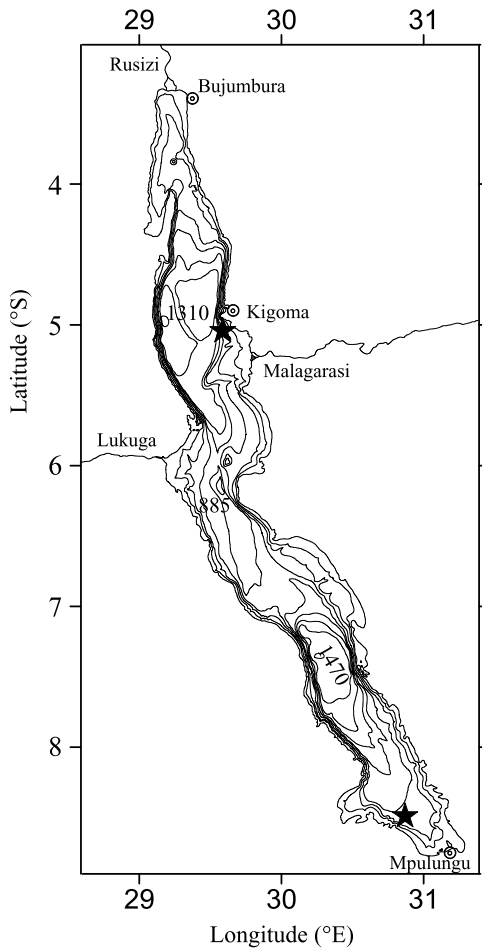


**Figure 1.** Lake Tanganyika. Isobaths are given every 250 m, and for 100 m and 1400 m. The deepest sites in the north, center, and south basins are indicated (1310, 885, and 1470 m, respectively). The rivers Malagarasi and Rusizi to the east and north, respectively, are the major inflows, while the lake is drained by the Lukuga River into the Congo basin. The positions of two buoys with data recorders in the north basin and at the south end of the lake are indicated by stars, and the three towns around the lake where shore stations were based are indicated.

has a maximum width of 48 km. The surface of the lake is 775 m above sea level. The lake has two deep basins (Figure 1), one in the north and one in the south, each over 1300 m deep. There are two main seasons, the cool, dry season, from May to September, and the warm wet season, from October to April [Verburg and Hecky, 2003]. Average annual air temperature in May 1995 to May 1996 was 25.3°C, with the average being about 0.4°C higher at the south basin compared with the north basin. Mean precipitation in the lake area is about 1000 mm yr<sup>-1</sup>.

### 3. Methods

#### 3.1. Sites and Sampling Methods

[7] Two buoys with sensors and data recorders were anchored about 5 km from shore in water circa 400 m deep in the north basin (14 km SW of Kigoma) and 40 km NW of

the south end of the lake (Figure 1). Equipment and sensors for automatic meteorological and hydrodynamic data collection are described in Table 1. Water temperature was recorded at the two buoys with thermistor strings and sensors at 11 different depths from 1 m to 300 m. The energy fluxes were calculated from measurements of wind speed and air temperature obtained from buoys in the north basin (hourly) and south basin (half hourly) and relative humidity, air pressure and solar radiation were obtained from the shore station at the north end of the lake (Bujumbura) for the north basin and at the south end (Mpulungu) for the south basin. All the data were collected as instantaneous values, except wind speed, which was recorded as the mean over the recording time interval. The threshold wind speed for the anemometer was 0.3 m s<sup>-1</sup>.

[8] At Bujumbura, meteorological sensors were placed at 4 m above water level on a jetty in the harbor. At Mpulungu, sensors were placed at 9.5 m height on a hill about 300 m inland. Buoy sensors were placed at 2.6 m above the lake surface. For the calculations of the energy fluxes in the south basin, the humidity data were adjusted to account for the difference with humidity measured overwater at the buoy in the south basin [Verburg and Hecky, 2003]. A linear relation was used between humidity at the land weather station and humidity at a jetty on the lake shore ( $r = 0.74$ ,  $n = 318$ ,  $P < 0.0001$ ). The adjusted humidity was similar to humidity measured at the buoy during cruises in 1996 and 1997 using Aanderaa humidity sensors (mean relative humidity 56% and 57%,  $n = 52$  simultaneous measurements, at the Mpulungu land station and at the Mpulungu buoy, respectively). With both buoys about 5 km offshore, the ratio of fetch to the sensor height was about 2000, well over the recommended minimum of 100 to 1000 [Hicks, 1975; Imberger and Patterson, 1989] to ensure that their position was within the developing internal boundary layer over the water.

#### 3.2. Calculations

[9] This paper focuses on latent ( $E$ ) and sensible heat ( $H$ ) fluxes but also estimates net radiation ( $Q$ ). The net surface flux is estimated by difference as

$$F_S = Q - E - H. \quad (1)$$

Advection of heat by rivers into and out of the lake, by evaporated volume and by rainfall [Schertzer et al., 2000] was ignored because these components are small (as indi-

**Table 1.** Automatic Recording Stations, Recording Intervals, Recording Periods, and Sensor Types<sup>a</sup>

Station <sup>b</sup>	Recording Interval (min)	Recording Period
Bujumbura <sup>1,2,3,4,5,6</sup>	10	Mar 1993 to Dec 1996
Kigoma <sup>1,2</sup>	10	Jul 1993 to Nov 1996
Kigoma buoy <sup>1,2,3,7</sup>	30	Mar 1994 to Nov 1996
Mpulungu buoy <sup>1,2,3,7</sup>	60	Mar 1993 to Nov 1996
Mpulungu <sup>1,2,3,4,5,6</sup>	10	May 1994 to Nov 1997

<sup>a</sup>From Aanderaa instruments.

<sup>b</sup>Superscript numbers denote the following sensor type, model number, and accuracy, respectively: 1: wind speed, 2740, ±0.2 m s<sup>-1</sup>; 2: wind direction, 3150/2864, ±5°; 3: air temperature, 3455/3145, ±0.1°C; 4: air pressure, 2810, ±0.2 mbar; 5: relative humidity, 3445, ±2%; 6: solar radiation, 2770, ±10 W m<sup>-2</sup>; and 7: water temperature, 2903, ±0.03°C.

cated by the long residence time of Lake Tanganyika of approximately 275 years [Verburg and Hecky, 2009].

[10] Net radiation is the sum of absorbed solar radiation  $S$  (short-wave) and net long-wave radiation  $L^*$ .  $L^*$  was estimated as the difference between the absorbed incoming and emitted outgoing long-wave radiative fluxes, which were estimated from air temperature, relative humidity, cloudiness and water surface temperature following Brutsaert [1982]. The latent and sensible heat fluxes are considered positive when there is a net loss of heat from the lake to the atmosphere and negative when heat is entering the lake.  $F_S$  is considered to account for the change in heat storage and is positive when the lake gains heat. The energy balance components were calculated hourly for the south basin and half hourly for the north basin for the period May 1995 to November 1996.

### 3.3. Bulk Aerodynamic Transfer Method

[11] Sensible and latent heat fluxes are linearly proportional to transfer coefficients, which vary with the local stability of the atmospheric boundary layer (ABL), which is affected by wind velocity and the gradients of temperature and humidity above the water surface. Our algorithm is similar to the types of algorithms that are typically used for the computation of ocean surface fluxes [Zeng *et al.*, 1998; Renfrew *et al.*, 2002; Fairall *et al.*, 2003]. The methods in earlier work on the Laurentian Great Lakes [Derecki, 1981; Croley, 1989; Lofgren and Zhu, 2000; Laird and Kristovich, 2002] are all based on the methods of Quinn [1979], without further modification. Our algorithm differs from that applied in studies on the Laurentian Great Lakes (mentioned above) by accounting for roughness lengths of temperature and vapor [Brutsaert, 1982], by allowing the roughness length of momentum to account for smooth flow [Zeng *et al.*, 1998; Smith, 1988], in the formulation of the stability functions for stable conditions [Imberger and Patterson, 1989], and by adjusting air density for temperature and air pressure.

[12] The measured variables used in the calculations are air temperature ( $T$ , °C), water surface temperature ( $T_o$ , °C), relative humidity ( $R_H$ , %), wind speed ( $U_Z$ , m s<sup>-1</sup>) and air pressure ( $p$ , mbar). Sensible heat and latent heat fluxes (W m<sup>-2</sup>) are estimated with bulk aerodynamic methods,

$$H = \rho_a C_a C_H U_Z (T_o - T) \text{ sensible heat transfer} \quad (2)$$

$$E = \rho_a L_V C_E U_Z (q_s - q_z) \text{ latent heat transfer,} \quad (3)$$

and evaporation (m s<sup>-1</sup>) is estimated as

$$E^* = E / \rho_w L_v, \quad (4)$$

where  $C_H$  and  $C_E$  are the transfer coefficients for sensible heat and latent heat, respectively,  $C_a$  is the specific heat of air (1005 J kg<sup>-1</sup> K<sup>-1</sup>) and

$$\rho_a = 100p/[R_a(T + 273.16)] \text{ air density, kg m}^{-3}, \quad (5)$$

$$R_a = 287(1 + 0.608 q_z) \text{ gas constant for moist air, J kg}^{-1} \text{ K}^{-1}, \quad (6)$$

$$L_V = 2.501 \times 10^6 - 2370 T_o \text{ latent heat of vaporization, J kg}^{-1}, \quad (7)$$

$$q_s = 0.622 e_{sat}/p \text{ specific humidity at saturation, kg kg}^{-1}, \quad (8)$$

$$q_z = 0.622 e_a/p \text{ specific humidity, kg kg}^{-1}, \quad (9)$$

$$e_{sat} = 6.11 \exp^{[17.27T_o/(237.3+T_o)]} \text{ saturated vapor pressure at } T_o, \text{ mbar,} \quad (10)$$

$$e_a = R_H e_s / 100 \text{ vapor pressure, mbar,} \quad (11)$$

$$e_s = 6.11 \exp^{[17.27T/(237.3+T)]} \text{ saturated vapor pressure at } T, \text{ mbar.} \quad (12)$$

Water density (kg m<sup>-3</sup>) is given by Henderson-Sellers [1986],

$$\rho_w = 10^3 \times (1 - 1.9549 \times 10^{-5}|T_o - 3.84|^{1.68}). \quad (13)$$

Neutral transfer coefficients (dimensionless) are computed from

$$C_{DN} = (u^*/U_Z)^2 = \{\kappa / [\ln(z/z_o)]\}^2 \text{ drag coefficient, neutral} \quad (14)$$

$$\begin{aligned} C_{EN} &= \kappa^2 / [\ln(z/z_o) \ln(z/z_E)] \\ &= \kappa C_{DN}^{1/2} / [\ln(z/z_E)] \text{ latent heat transfer coefficient, neutral,} \end{aligned} \quad (15)$$

and the transfer coefficient for sensible heat ( $C_{HN}$ ) is assumed the same as for latent heat [Zeng *et al.*, 1998],

$$C_{HN} = C_{EN}, \quad (16)$$

where  $z$  is the measurement height (2.6 m),  $\kappa$  is the von Karman constant (0.41) and  $g$  is the gravitational acceleration (9.81 m s<sup>-2</sup>). Air shear velocity (m s<sup>-1</sup>) is estimated by

$$u^* = (C_D U_Z^2)^{1/2} = \kappa U_Z / [\ln(z/z_o)], \quad (17)$$

and the roughness lengths are given by

$$z_o = (\alpha u_*^2 / g) + (0.11\nu/u_*) \text{ roughness lengths for momentum, m} \quad (18)$$

$$z_E = z_o \exp(-2.67 Re^{1/4} + 2.57) \text{ roughness length for vapor, m,} \quad (19)$$

where  $\alpha$  is the Charnock constant (0.013, following Zeng *et al.* [1998]), and

$$Re = u^* z_o / \nu \text{ roughness Reynolds number.} \quad (20)$$

Roughness lengths for temperature ( $z_T$ ) and for vapor are assumed the same [Zeng *et al.*, 1998],

$$z_T = z_E. \quad (21)$$

Kinematic viscosity of air ( $\text{m}^2 \text{s}^{-1}$ ) can be obtained as

$$\nu = \mu / \rho_a, \quad (22)$$

where dynamic viscosity of air ( $\mu$ ) is given by the linear relation with air temperature (estimated using data from Montgomery [1947];  $R^2 = 1.0$ ,  $n = 7$ ,  $P < 0.00001$ ),

$$\mu = 4.94 \times 10^{-8} T + 1.7184 \times 10^{-5}, \text{ kg m}^{-1} \text{s}^{-1}. \quad (23)$$

[13] We initialized  $u^*$  from wind speed at 10 m ( $U_{10}$ ) using work of Amorocho and De Vries [1980],

$$u_* = U_{10} (0.0015 \{1 + \exp[(-U_{10} + 12.5)/1.56]^{-1}\} + 0.00104)^{-2}, \quad (24)$$

and then conducted a simple iteration loop by computing the roughness length for momentum  $z_o$ , using this to compute  $u^*$  (equation (17)). This was fed back into the roughness length for momentum until it converged to within 0.001% of the previous value of  $z_o$ , followed by the calculation of the neutral transfer coefficients.  $U_{10}$  is estimated by [Schertzer *et al.*, 2003]

$$U_{10} = U_z (10/z)^{1/7} \quad (25)$$

and after obtaining  $z_o$  by

$$U_{10} = U_z \ln(10/z_o) / [\ln(z/z_o)]. \quad (26)$$

### 3.4. Adjustment of Transfer Coefficients for Atmospheric Stability

[14] Atmospheric stability is a function of the Obukhov stability length  $L$  (m),

$$L = \frac{-\rho_a u_*^3 T_V}{\kappa g \left( \frac{H}{C_a} + 0.61 \frac{(T + 273.16)E}{L_V} \right)}, \quad (27)$$

which is a measure of the ratio of the reduction of potential energy due to wind mixing and the growth of atmospheric stratification due to the heat flux [Brutsaert, 1982]. When  $L$  is negative the boundary layer is convective and vertical transport is enhanced. This is expressed by higher transfer coefficients. The opposite is true for stable stratified boundary layers ( $L > 0$ ) when the heat and latent fluxes are reduced. In the neutral case,  $L = \infty$  or  $-\infty$ , the stability parameter

$$\zeta = z L^{-1} = 0, \quad (28)$$

and the atmospheric transfer coefficients are equal to their neutral values.

[15] The virtual air temperature (K) is given by

$$T_V = (T + 273.16)[1 + 0.61q_Z] \quad (29)$$

and the virtual temperature of saturated air at the water surface (K) by

$$T_{oV} = (T_o + 273.16)[1 + 0.61q_S], \quad (30)$$

while the virtual air-surface temperature difference is given by

$$\Delta\theta = T_{oV} - T_V. \quad (31)$$

[16] The stability of the atmosphere above the water surface is accounted for in the mass transfer formulas by adjusting the transfer coefficients using the atmospheric stability functions ( $\Psi$  functions [Brutsaert, 1982]) that were first developed by Dyer [1967], Businger *et al.* [1971] and others. There are different sets of  $\Psi$  functions for stable and unstable conditions to adjust the transfer coefficients for stability,

Stability functions for  $\zeta > 0$  (stable atmosphere)

$$\Psi_M = \Psi_T = \Psi_E = -5 \zeta \quad (0 < \zeta < 0.5), \quad (32a)$$

$$= 0.5 \zeta^{-2} - 4.25 \zeta^{-1} - 7 \ln \zeta - 0.852 \quad (0.5 < \zeta < 10), \quad (32b)$$

$$= \ln \zeta - 0.76 \zeta - 12.093 \quad (\zeta > 10), \quad (32c)$$

Stability functions for  $\zeta < 0$  (unstable atmosphere)

$$\Psi_M = 2 \ln[(1+X)/2] + \ln[(1+X^2)/2] - 2 \arctan X + \pi/2, \quad (33a)$$

$$\Psi_T = \Psi_E = 2 \ln[(1+X^2)/2], \quad (33b)$$

$$X = (1 - 16\zeta)^{1/4}. \quad (33c)$$

Stability dependent transfer coefficients are obtained as

$$C_D = \kappa^2 / [\ln(z/z_o) - \Psi_M]^2 \text{ drag coefficient}, \quad (34)$$

$$C_E = \kappa^2 / \{[\ln(z/z_o) - \Psi_M][\ln(z/z_E) - \Psi_E]\} \\ = \kappa C_D^{1/2} / [\ln(z/z_E) - \Psi_E] \text{ latent heat coefficient}, \quad (35)$$

$$C_H = C_E \text{ sensible heat coefficient}. \quad (36)$$

[17] Because  $L$  and therefore the  $\Psi$  functions are defined as functions of  $E$  and  $H$ , the calculations of  $E$  and  $H$  are initiated with neutral fluxes  $E_N$  and  $H_N$  (by using  $C_{DN}$  and  $C_{EN}$ ) and solved by iteration until the values converged [Hicks, 1975; Renfrew *et al.*, 2002]. In each iteration  $u_*$ ,  $z_o$ ,  $z_T$ ,  $z_E$ , the drag and transfer coefficients and  $H$  and  $E$  were recalculated and used to recalculate  $L$  and the  $\Psi$  functions. The stability calculations were iterated until  $L$  converged to within 0.001% of the previous  $L$ : generally ten iterations were sufficient. Bounds on  $|\zeta|$  (suggested by Imberger and Patterson [1989] and MacIntyre *et al.* [2002]) were not

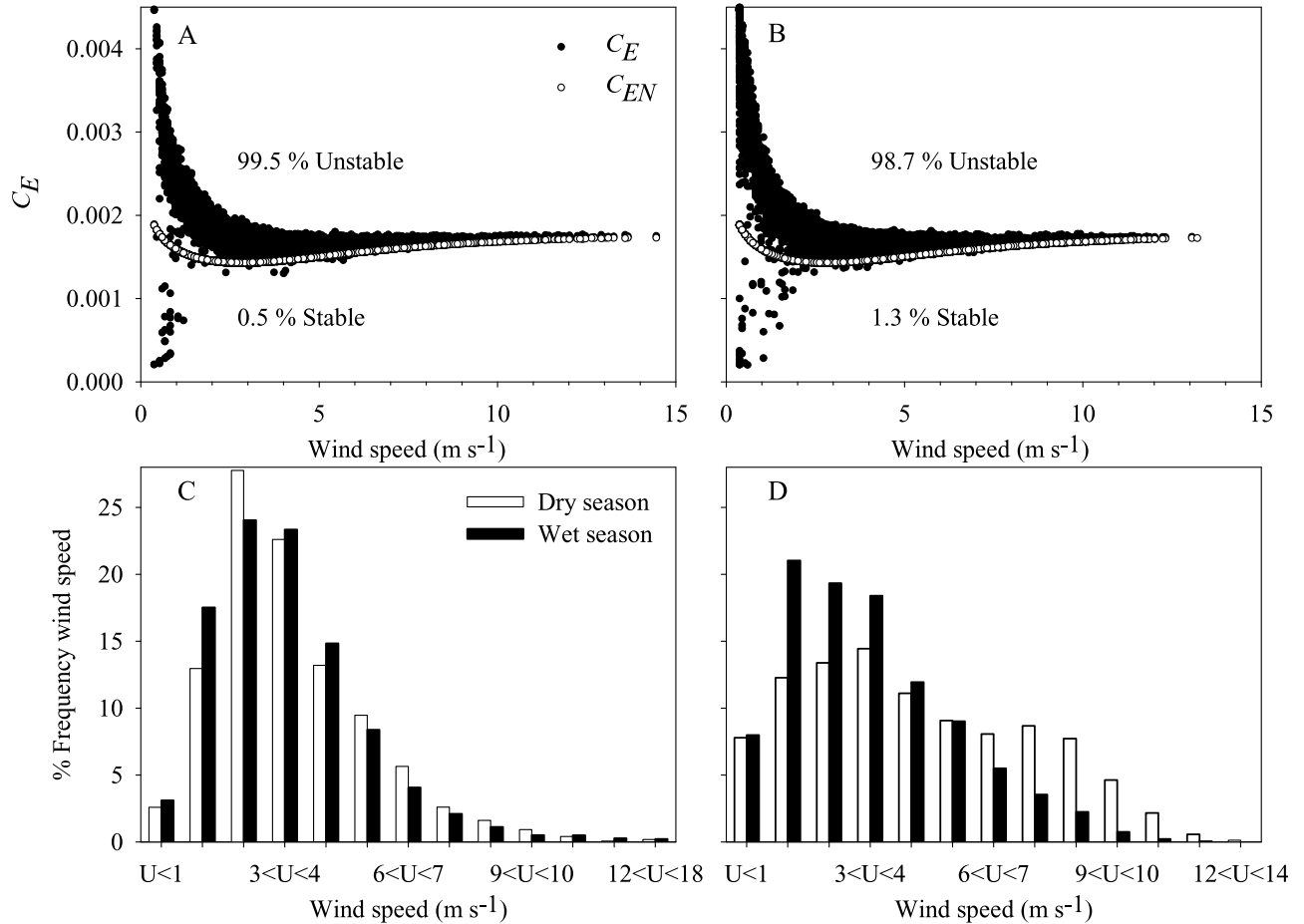


**Figure 2.** Dependence of the transfer coefficient  $C_E$  on wind speed. The ABL is unstable when  $C_E$  is higher than  $C_{EN}$  and stable when  $C_E$  is lower than  $C_{EN}$ . (a) Half-hourly values for the north basin ( $n = 27,424$ ). (b) Hourly values for the south basin ( $n = 11,898$ ). Frequency distribution of hourly mean wind speeds between March 1993 and November 1996 (c) at the buoy in the north basin ( $n = 32,791$ ) and (d) at the buoy at the south end of the lake ( $n = 31,881$ ), the most windy of the five stations (Table 1).

imposed because  $C_E$ ,  $H$  and  $E$  did not behave erratically at extreme values of  $\zeta$ , although more iterations were necessary to resolve the few extreme stable cases, as was earlier reported by *Smith* [1988] and *Fairall et al.* [1996].

## 4. Results

### 4.1. Roughness Lengths

[18] The momentum roughness length  $z_o$  averaged  $6 \times 10^{-5} m$  and increased strongly with wind speed similar to the relationship shown by *Renfrew et al.* [2002]. The  $z_E$  did not vary significantly and was about  $8 \times 10^{-5} m$  and decreased slightly at wind speeds over  $7 m s^{-1}$ . The relationship of  $z_E$  with wind speed agreed with results of *Katsaros* [1998] and *Renfrew et al.* [2002] although  $z_E$  was here on average slightly higher as a result of higher air temperatures.

### 4.2. Effects of Atmospheric Stability

[19] The average of the neutral drag coefficient was  $1.44 \times 10^{-3}$  and increased strongly and linearly with wind speeds above  $2 m s^{-1}$  ( $C_{DN} = 1.32 \times 10^{-3}$  at  $U_z = 2 m s^{-1}$  and  $C_{DN} =$

$2.48 \times 10^{-3}$  at  $U_z = 14.5 m s^{-1}$ ) as expected [*Renfrew et al.*, 2002]. The stability function increased the average drag coefficient by 15% to  $1.66 \times 10^{-3}$ .

[20] The neutral transfer coefficient for heat and for moisture  $C_{EN}$  was on average  $1.50 \times 10^{-3}$  and increased with wind speeds  $> 2 m s^{-1}$  (Figures 2a and 2b) but less than the neutral drag coefficient which agreed with results from *Fairall et al.* [2003] and *Renfrew et al.* [2002]. *Zeng et al.* [1998] found  $C_{EN}$  increasing for wind speeds from 3 to  $12 m s^{-1}$ , and constant at wind speeds from 12 to  $20 m s^{-1}$ . In addition, the increase in  $C_{EN}$  with decreasing wind speeds below  $2 m s^{-1}$  agreed with results of *Fairall et al.* [2003, 1996].  $C_{EN}$  varies with the roughness lengths (section 3.2.4). The larger the roughness lengths, the larger the transfer coefficients and the mass fluxes. The effect of increasing  $z_o$  on  $C_{EN}$  when wind speed increases is partly canceled by a decrease in  $z_T$  and  $z_E$  with increasing wind speed. Measurements were here recorded at  $2.6 m$ , not at  $10 m$  height as in most atmospheric studies on the ocean, which affects the magnitude of  $C_{DN}$  and  $C_{EN}$ . The neutral transfer coefficients were similar to literature values when corrected for measurement height following the method of *Amoracho and De*

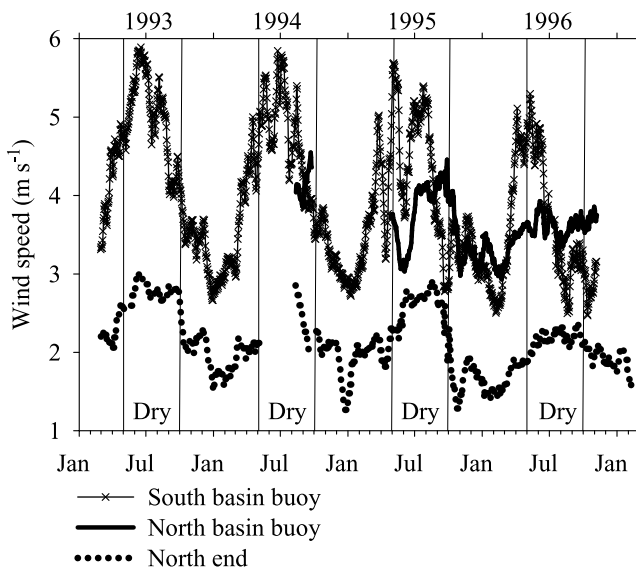


**Figure 3.** Wind speed at the north end of the lake and in the north and south basins in 1993 to 1996 with dry seasons indicated (21 day moving averages).

*Vries* [1980] [*MacIntyre et al.*, 2002]. An approximate conversion of transfer coefficients at 2.6 m height to coefficients at 10 m height can be derived from *Amorocho and De Vries* [1980],

$$C_{X10} = 0.368 \times C_{X2.6}^{0.884}. \quad (37)$$

Examples of means given for  $C_{EN}$  at 10 m in literature are  $1.35 \times 10^{-3}$  [*Fisher et al.*, 1979; *Imberger and Patterson*, 1989],  $1.2 \times 10^{-3}$  [*Smith*, 1988] and  $1.15 \times 10^{-3}$  [*Fairall et al.*, 2003] which translate to  $1.76 \times 10^{-3}$ ,  $1.54 \times 10^{-3}$  and  $1.47 \times 10^{-3}$ , respectively, at 2.6 m.

[21] The ABL at Lake Tanganyika was most of the time unstable ( $\zeta < 0$  occurred 99.1% of the time in May 1995 to May 1996), resulting in enhancement of transfer coefficients and heat fluxes. The stability functions increased the average transfer coefficient  $C_E$  by 23% to  $1.85 \times 10^{-3}$ . The stability effect on the transfer coefficient was largest when wind speeds were low and when the virtual air-surface temperature difference  $\Delta\theta$  was large, both in the unstable ABL (enhanced transfer) and stable ABL (reduced transfer for  $E$  and  $H$ ; negative transfer for  $H$ ). The effect of wind speed on the stability adjusted transfer coefficient is illustrated by Figures 2a and 2b with  $C_E$  converging to  $C_{EN}$  with increasing wind speed, as  $\zeta$  converged to zero. At Lake Tanganyika wind speeds are usually low, rarely over  $10 \text{ m s}^{-1}$  (Figures 2c and 2d).

[22] Annual mean  $C_E$  in the south basin ( $0.00192$ ) was significantly higher ( $p < 0.00001$ ) than in the north basin ( $0.00177$ ) and the mean difference between minimum and maximum values per 24 h in the south basin ( $78\% \pm 43$  of the annual mean) was significantly higher ( $p < 0.00001$ ) than in the north basin ( $56\% \pm 30$  of the annual mean). The mean difference between hourly and daily mean  $C_E$  as a percentage of the daily mean was similar to the mean difference between the daily means and annual mean  $C_E$  as a percentage of the annual mean ( $14\% \pm 18$  and  $13\% \pm 13$ ,

respectively, in the south basin, and  $8\% \pm 10$  and  $5\% \pm 4$ , respectively, in the north basin) but significantly different ( $p < 0.00001$ ) between basins.

#### 4.3. Transfer Coefficients and Relevant Relationships

[23] Wind speeds decreased along the length of the lake from south to north (Figure 3) and were predominantly from the south to southeast throughout the year [Verburg and Hecky, 2003]. Wind speeds were highest during the cool dry season (Figure 3). Relative humidity was at a minimum in August–September and maximum in March, in both basins. Relative humidity was higher on average in the north basin ( $74\% \pm 10 \text{ SD}$ ) than in the south ( $59\% \pm 7 \text{ SD}$ ), probably because of the downwind effect of evaporation along the length of the lake (rainfall was highest at the south end). The seasonal effect of relative humidity on  $\Delta\theta$  was opposite to the effect of  $T_o - T$ .

[24] Monthly wind speed and  $\Delta\theta$  (Figure 4) were inversely correlated ( $r = 0.45$ ,  $p < 0.005$ ).  $\zeta$  depends on both wind speed and  $\Delta\theta$  and  $|\zeta|$  was large when wind speed was low (north basin:  $r = -0.77$ ,  $p < 0.0001$ ; south basin:  $r = -0.67$ ,  $p < 0.001$ ) and was large when  $\Delta\theta$  was high (north basin:  $r = 0.70$ ,  $p < 0.001$ ; south basin:  $r = 0.47$ ,  $p < 0.05$ ), generally in the warm wet season. The stability adjusted transfer coefficients closely tracked  $\zeta$  as expected ( $C_E$ :  $r = 0.99$ ,  $p < 0.00001$ ;  $C_D$ :  $r = 0.84$ ,  $p < 0.00001$ ). The atmosphere was more unstable and the mean transfer coefficients were higher in the south basin (mean  $\zeta = -1.28$ ) than in the north basin (mean  $\zeta = -0.55$ ), although mean wind speeds were higher in the south basin. This was probably explained by a higher frequency of low wind speeds ( $< 2 \text{ m s}^{-1}$ ) at the south basin (Figure 2). Both  $C_E$  and  $C_D$  increased with wind speeds decreasing below about  $2 \text{ m s}^{-1}$ .

#### 4.4. Heat Fluxes

[25] Temperature of the water surface generally was low when the combined heat loss by  $H$  and  $E$  was high (Figure 4). While the annual mean  $C_E$  (May 1995 to May 1996) was 23% higher than the mean  $C_{EN}$ , the annual mean  $E$  was enhanced less, by 13% relative to  $E$  with an assumed neutral ABL (Table 2) because the effect of atmospheric stability on  $C_E$  was highest at low wind speeds, when  $E$  is small.

[26] The differences between estimated neutral and stability adjusted values of  $E$  and  $H$  were significant (paired  $t$  test,  $t = 171$ ,  $df = 7537$ ,  $p = 0$  for the difference between  $E$  and  $E_N$ , and a similar result for the sensible heat flux). Error estimates of the annual mean estimates of  $E$  and  $H$  were derived from the accuracies of the 5 sensor types combined (wind speed, humidity, air and water temperature, air pressure) which were involved in the estimation of  $E$  and  $H$ , over 100 realizations. For each sensor, a random offset was chosen by applying an uncertainty to the measurements equal to the sensor accuracy, and the offset was kept constant for the whole record, thereby creating a measurement bias (as opposed to random measurement error which would reduce to zero in the annual averaged fluxes [*Fairall et al.*, 1996]). The fluxes were then computed for each time step based on this offset (with a different offset for each sensor), and the annual mean was derived. This was repeated 100 times (using Matlab). The standard deviations of the annual mean  $E$  for the north and south basins were

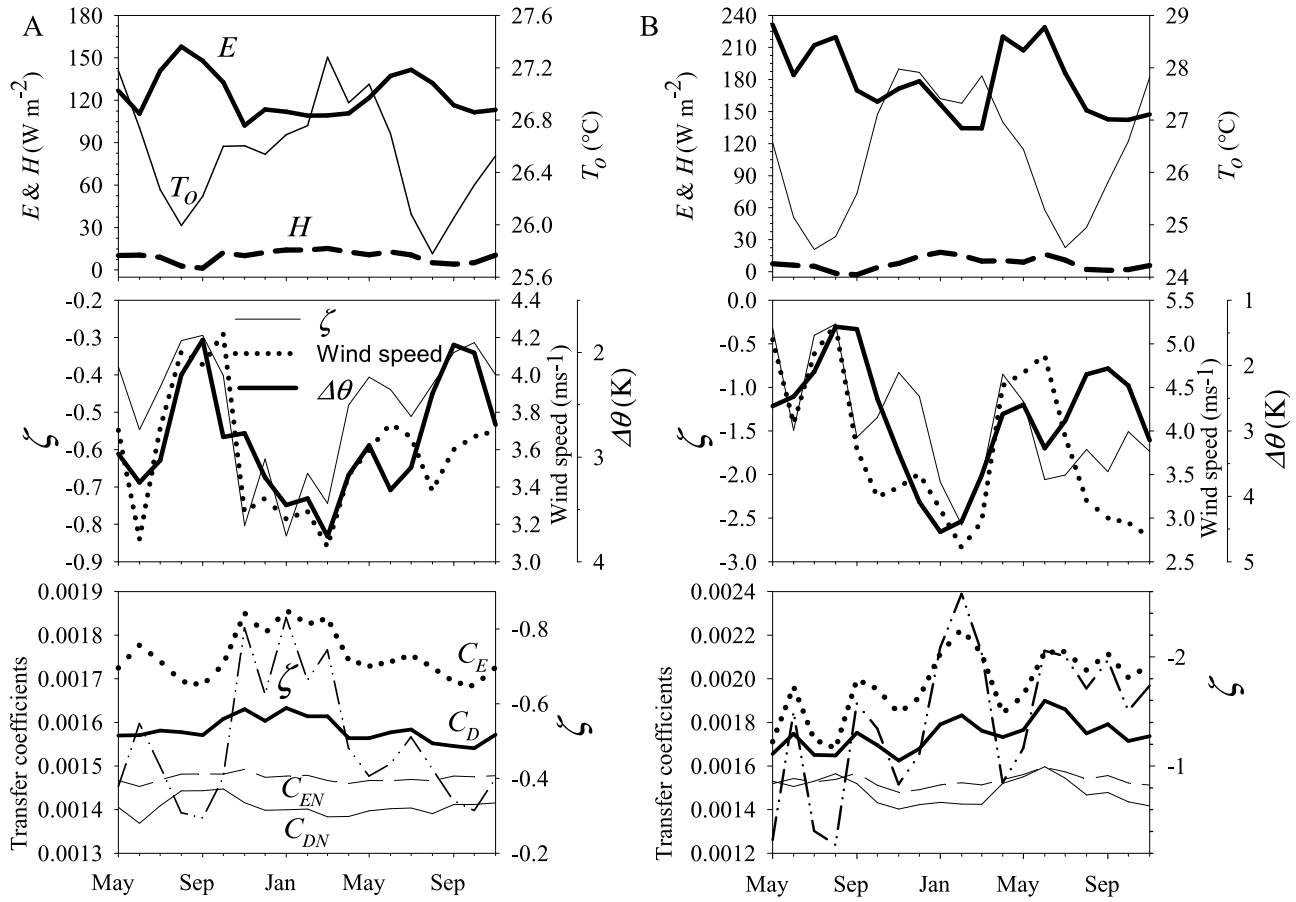


**Figure 4.** Monthly mean  $E$ ,  $H$ ,  $T_o$ , wind speed,  $\Delta\theta$ ,  $\zeta$ , and transfer coefficients. (a) North basin. (b) South basin. Note inverted scales for  $\Delta\theta$  and  $\zeta$  in several of the plots and differences in scales between Figures 4a and 4b.

2.9% and 2.8% of the mean, respectively. The standard deviations of the annual mean  $H$  for the north and south basins were 4.6% and 5.9% of the mean, respectively.

[27] Using daily or annual mean data inputs underestimated  $E$  by 4 to 5% ( $p < 0.00001$ , paired  $t$  test for the daily mean data inputs), relative to the results achieved using hourly data (Table 3). There was no seasonality to the differences in results achieved with daily mean inputs and hourly inputs. Using neutral transfer coefficients (which vary with wind speed), and ignoring atmospheric stability, underestimated  $E$  by 11 and 13% in the north and south basins, respectively. With transfer coefficients assumed constant and taken from the literature ( $C_E = C_H = 1.35 \times 10^{-3}$  referenced to 10 m [MacIntyre *et al.*, 2002]), and adjusted for measurement height following MacIntyre *et al.* [2002] and Amoroch and De Vries [1980],  $E$  was overestimated by 3% relative to the results achieved with stability accounted for by stability functions. Higher long-term average transfer coefficients suggested in literature (e.g.,  $1.9 \times 10^{-3}$  referenced to 10 m, from a literature summary by Imberger and Patterson [1989]) would overestimate  $E$  much more.

[28] Highly stable or unstable conditions ( $|\zeta| > 15$ ) occurred only when wind speeds were very low (average  $0.4 \text{ m s}^{-1}$ ), near the threshold wind speed of the sensor. Because latent and sensible heat fluxes are proportional to

wind speed (section 3.3, equations (2) and ((3))) the fluxes were small under highly stable or unstable conditions.

#### 4.5. Stability of the ABL

[29] Water temperatures were on average  $1.56$  and  $0.93^{\circ}\text{C}$  above air temperatures in the north and south basins, respectively. Mean temperature differences between the water surface and the air were least in August to October, and at midday could become negative, occasionally allowing stable conditions to develop. Stable conditions were most frequent in those months, with monthly mean relative frequency of stable conditions of up to 2 and 5% in the north and

**Table 2.** Comparison of Annual Mean Neutral and Stability-Dependent Drag and Transfer Coefficients Along With  $E$  and  $H$ <sup>a</sup>

	$C_{DN}$	$C_{EN}$	$E_N$	$H_N$	$C_D$	$C_E$	Differences			
							$E$	$H$	$C_D$	$C_E$
North basin	1.41	1.47	107.1	8.7	1.59	1.77	122.5	10.2	13%	20%
South basin	1.48	1.52	164.7	6.1	1.72	1.92	183.7	7.2	16%	26%
Mean	1.44	1.50	135.9	7.4	1.66	1.85	153.1	8.7	15%	23%

<sup>a</sup>Height: 2.6 m.  $E$  and  $H$  units:  $\text{W m}^{-2}$ .  $C_{D(N)}$  and  $C_{E(N)}$  are  $\times 10^{-3}$ . Differences are relative to the values for the neutral case.

**Table 3.** Annual Mean Latent and Sensible Heat Fluxes<sup>a</sup>

	North Basin				South Basin			
	E	Error ± SD	H	Error ± SD	E	Error ± SD	H	Error ± SD
This study	122.5		10.2		183.7		7.2	
Daily mean input data	117.7	-4.8 ± 4.6	9.7	-0.5 ± 1.4	175.8	-7.8 ± 6.1	5.6	-1.6 ± 2.0
Annual mean input data	116.6	-5.9	9.8	-0.4	175.3	-8.3	7.2	0.0
Neutral stability	107.1	-15.5 ± 3.3	8.7	-1.5 ± 0.8	164.7	-18.9 ± 7.7	6.1	-1.1 ± 1.3
$C_{EN} = 0.00135$ (constant)	126.3	+3.8 ± 4.5	10.3	+0.1 ± 0.3	188.8	+5.2 ± 10.6	7.0	-0.2 ± 0.6

<sup>a</sup>Unit is  $\text{W m}^{-2}$ . Results are compared with methods using (1) daily or (2) annual mean data inputs, (3) ignoring atmospheric stability and using neutral transfer coefficients (not constant but varying with wind speed), and (4) with neutral transfer coefficients assumed constant ( $C_{EN} = C_{HN} = 1.35 \times 10^{-3}$  at 10 m, adjusted for measurement height). Error is the difference relative to the results achieved using hourly data and with atmospheric stability accounted for. Standard deviations of the errors are given for the daily means of estimates.

south basin, respectively (Figure 5). Most of the rest of the year unstable conditions prevailed more than 99% of the time.

[30] The atmosphere in the boundary layer is only unstable when the virtual temperature of air (rather than the absolute air temperature) decreases with increasing height above the water surface (Figure 6). When  $T_o - T = 0$ , the atmosphere is unstable, unless relative humidity is 100% (at which the atmosphere is neutral). In Lake Tanganyika, the atmosphere could be unstable even with air temperatures higher than the water surface by about 1 to 2°C (Figure 6). The annual mean  $\Delta\theta$  was more similar between the north and south basins (2.99 and 2.83°K, respectively) than the annual mean  $T_o - T$  (1.56 and 0.93°C, respectively) as a result of lower relative humidity at the south basin compared with the north basin (Figure 5). Part of the difference between  $\Delta\theta$  and  $T_o - T$  is due to the effect of lower air pressure at the elevation of Lake Tanganyika (mean 921 mbar), compared with sea level, feeding back into the calculation of specific humidity.  $\Delta\theta$  is slightly higher at air pressures below that at sea level for the same value of  $T_o - T$ . The effect of altitude on  $\Delta\theta$  increases with decreasing humidity and increasing  $T_o - T$ , which would increase the incidence of unstable events.

[31] The ratio of the stability adjusted transfer coefficients to the neutral coefficients  $C_E/C_{EN}$ , was  $> 1$  when  $\Delta\theta$  was positive and the atmosphere was unstable, but was otherwise uncorrelated with  $\Delta\theta$  on hourly basis. The change in the proportional adjustment of the coefficients with  $\zeta$  was rapid for  $\zeta$  close to zero and tapered off for increasing  $|\zeta|$  (Figure 7). The correction of  $C_D$  at  $\zeta = -1$  or  $+1$  was +23% and -50% in the unstable and stable case, respectively, and the correction of  $C_E$  at  $\zeta = -1$  or  $+1$  was +34% and -51% in the unstable and stable case, respectively (Figure 7), much larger than the 10% found by Imberger and Patterson [1989]. The ratio  $C_E/C_{EN}$  was larger for unstable conditions than  $C_D/C_{DN}$  (Figure 7).

[32] While the stability adjustment of the transfer coefficient was largest at high  $|\zeta|$  (Figure 7), strong heat loss by evaporation ( $>200 \text{ W m}^{-2}$ ) only occurred when  $\zeta$  was close to zero due to the effect of high wind speeds. Stability  $\zeta$  was between -1 and zero 87.4% and 78.0% of the time in the north and south basins, respectively. Evaporation was a strong linear function of wind speed ( $R^2 = 0.79$  and 0.95 in the north and south basins, respectively).

#### 4.6. Effects of Local Values of $L_v$ , $\rho_a$ , and $\nu$ on Heat Fluxes and Stability

[33] Sensible and latent heat fluxes are proportional to air density, which was on average 10% lower at Lake Tanganyika (1.07  $\text{kg m}^{-3}$  at 25°C) than at sea level (1.17  $\text{kg m}^{-3}$  at 25°C) because of the lower air pressure at 775 m altitude (mean 924 mbar). In addition, high air temperatures in the tropics result in relative low air density. Compared with conditions at Lake Tanganyika, typical values of air density for temperate low-altitude lakes such as the Laurentian lakes would overestimate  $E$  by 14% (Table 4). Kinematic vis-

cosity ( $1.07 \text{ kg m}^{-3}$  at 25°C) than at sea level (1.17  $\text{kg m}^{-3}$  at 25°C) because of the lower air pressure at 775 m altitude (mean 924 mbar). In addition, high air temperatures in the tropics result in relative low air density. Compared with conditions at Lake Tanganyika, typical values of air density for temperate low-altitude lakes such as the Laurentian lakes would overestimate  $E$  by 14% (Table 4). Kinematic vis-

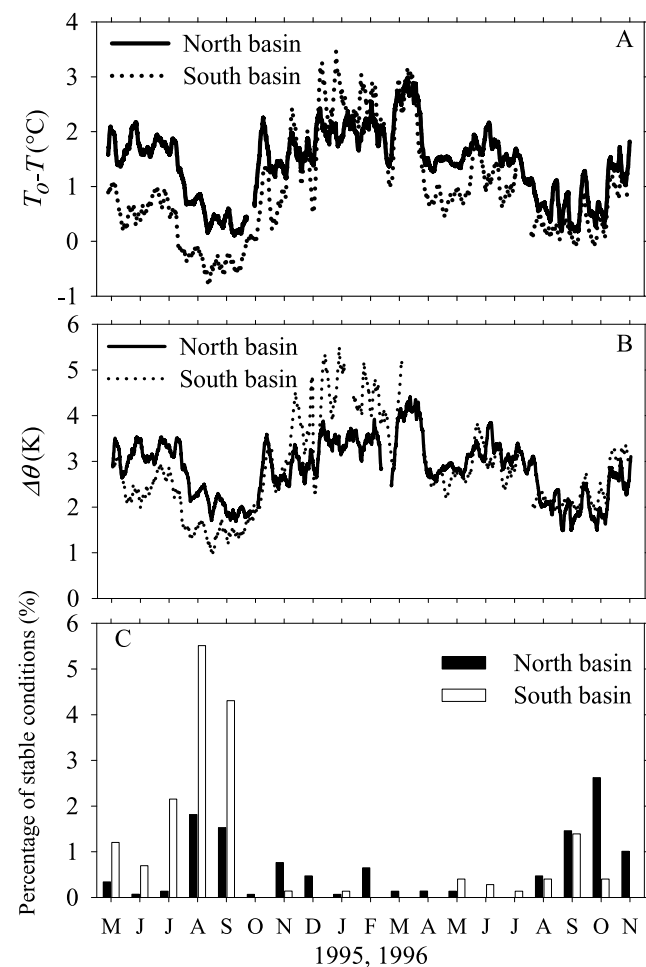


**Figure 5.** (a) Difference between water ( $T_o$ ) and air temperature ( $T$ ) for the north and south stations, using a 7 day moving average. (b) Difference between virtual water and air temperature for the north and south stations, using a 7 day moving average. (c) Percentage of days when stable conditions are present, averaged over each month.

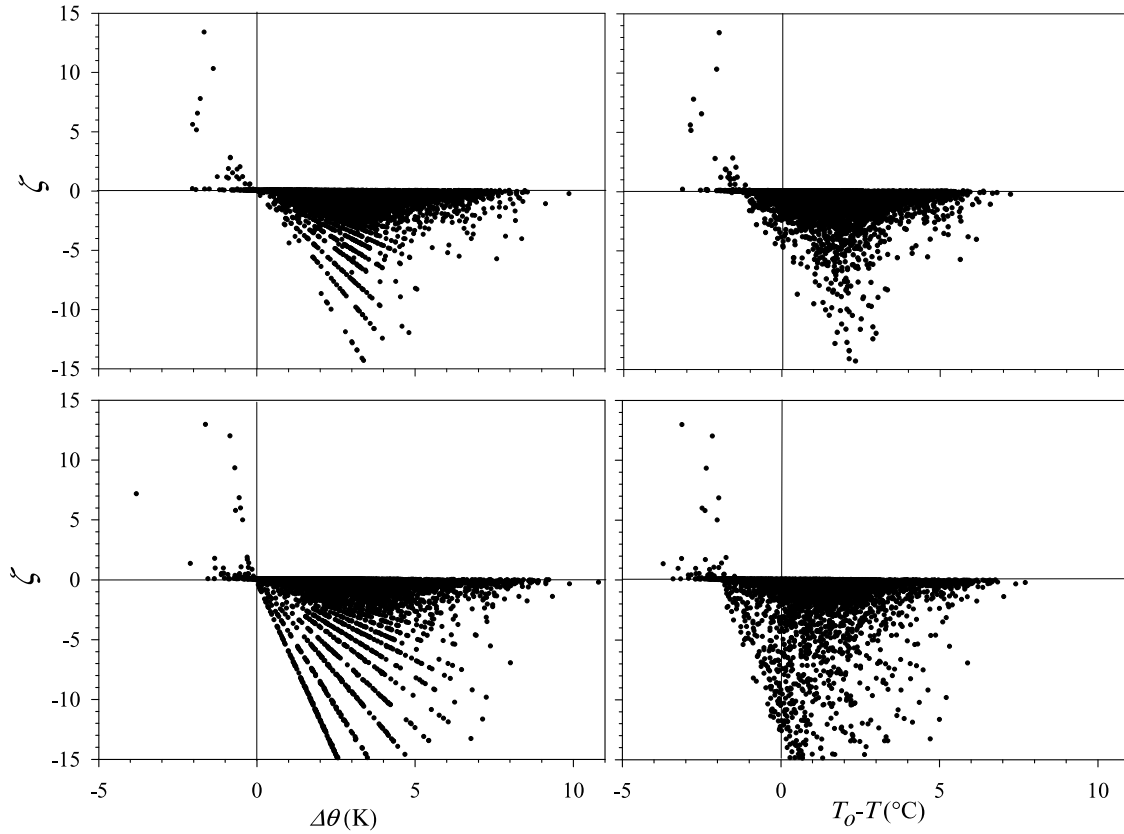


**Figure 6.** Relationships between  $\Delta\theta$  and  $T_o - T$  and  $\zeta$ . (top) North basin. (bottom) South basin. The regular pattern in  $\Delta\theta$  versus  $\zeta$  is an artifact caused by the precision of the input data.

cosity of air  $\nu$  is 18% lower at  $T = 10^\circ\text{C}$  and  $p = 1013$  mbar compared with conditions at Lake Tanganyika (Table 4). Such a low value of  $\nu$  would result in a 2% reduction of the estimate of  $E$ . Temperate values of  $L_V$  would result in an overestimate of 2% of  $E$ . The effects of temperate low-altitude values of  $\rho_a$ ,  $L_V$  and  $\nu$  on the transfer coefficient  $C_E$  were smaller than the effect on  $E$ , resulting in a decrease of up to 3%.

[34] Because neutral values are affected at similar rates as stability dependent values, the stability effects on  $E$  as expressed by the ratios to the neutral values are not much affected, they decrease by about 1% (Table 4). Results for the north and south basin were similar.

## 5. Discussion

### 5.1. Effects of Local Values of $L_V$ , $\rho_a$ , and $\nu$

[35] The extent to which the local, tropical values of  $\rho_a$ ,  $L_V$  and  $\nu$  affect the heat fluxes is substantial (Table 4). It is clear that unless  $\rho_a$ ,  $\nu$  and  $L_V$  are adjusted for air pressure and air temperature, estimates of the heat fluxes will be unrealistic at Lake Tanganyika. However, in the literature, air density is sometimes assumed constant as  $1.2 \text{ kg m}^{-3}$  [Lofgren and Zhu, 2000; Laval *et al.*, 2003]. The value of kinematic viscosity of air is usually set to a constant between  $14$  to  $15 \times 10^{-5} \text{ m s}^{-1}$  [Renfrew *et al.*, 2002]. The value of latent heat of vaporization is sometimes assumed constant [Lenters *et al.*, 2005]. Adopting typical temperate

values of  $\rho_a$ ,  $\nu$  and  $L_V$  for a tropical lake at 775 m altitude would result in an overestimation of 16% of annual mean  $E$ . The suggested values of  $1.2 \text{ kg m}^{-3}$  for  $\rho_a$  and  $14$  to  $15 \times 10^{-5} \text{ m s}^{-1}$  for  $\nu$  may be valid for average conditions in temperate low-altitude locations and realistic on an annual basis in the Laurentian lakes. However, it is important to note that while these constant values may be similar to the annual means of  $\rho_a$  and  $\nu$  at the Laurentian lakes,  $\rho_a$  and  $\nu$  are not constant at the Laurentian lakes either, with much larger differences between summer and winter than in the tropical and fairly constant conditions of Lake Tanganyika. Adopting constants for  $\rho_a$  and  $\nu$  will cause various large bias effects, not only in the tropics and at higher altitude, but also in nonaverage conditions such as during winter and summer at the Laurentian lakes.

### 5.2. Evaluation of Heat Flux Results

[36] Annual mean  $E$ ,  $H$  and  $Q$  were estimated over a period of 1 year chosen from the data set such that heat content in the water column determined by the thermistors was the same at the end as it was at the start of the period (therefore the annual mean  $F_s = 0$ ). The annual mean net radiation was  $161.4 \text{ W m}^{-2}$ . The mean net surface flux  $F_s$  calculated on an hourly basis over the same 1 year period by difference from  $Q$ ,  $E$  and  $H$  (equation (1)) was 0.2% of net radiation. In other words, our study managed to account for nearly all input heat in terms of heat loss and compares well with results in other Great Lakes where the unexplained

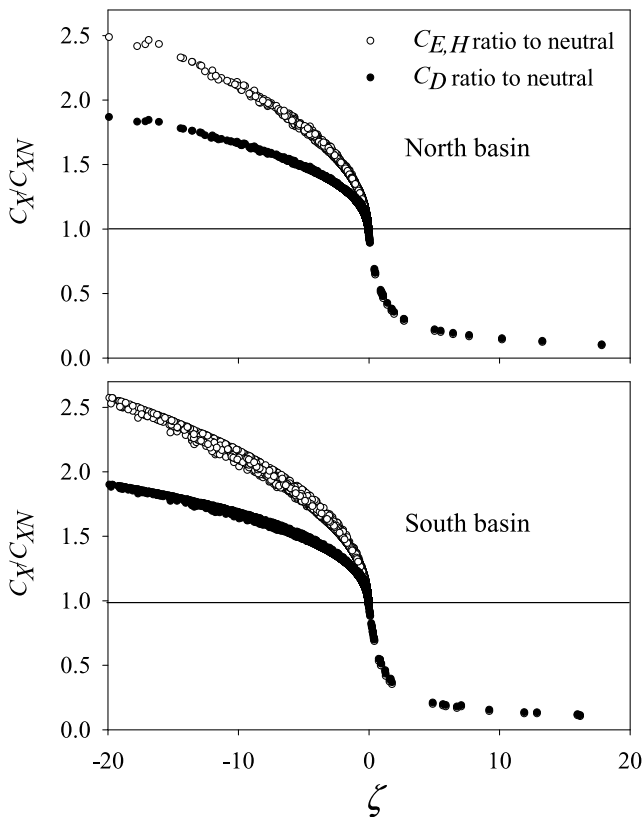


**Figure 7.** Relationship between the stability parameter  $\zeta$  and the ratio of the stability adjusted transfer coefficients  $C_E$  and  $C_D$  to the respective neutral coefficients.

annual residual ranged from 4 to 51% of the net radiation (mean 17% for the 5 Laurentian lakes) in spite of complete areal coverage by using remotely sensed water temperatures [Lofgren and Zhu, 2000].

[37] The mean Bowen ratio of  $H/E$  was 0.06 (0.08 in the north basin and 0.04 in the south basin), which is very low compared with temperate lakes. The stability of the atmosphere does not affect the Bowen ratio because the transfer coefficients cancel out by dividing  $H$  by  $E$ . The Bowen ratio ranges in the North American Great Lakes from 0.37 for Lake Erie, the southernmost lake, where  $E$  is largest ( $45.4 \text{ W m}^{-2}$  [Lofgren and Zhu, 2000]), to 1.10 for Lake Superior ( $E = 30.3 \text{ W m}^{-2}$  [Lofgren and Zhu, 2000]). As a result of high tropical water temperatures,  $E$  was much larger in Lake Tanganyika than in the North American Great Lakes, while  $H$  was smaller.  $E$  was from 3.4 times larger than in Lake Erie, to 5.0 times larger than in Lake Superior.  $H$  was from 0.52 times that in Lake Erie, to 0.26 times that in Lake Superior [Lofgren and Zhu, 2000]. The relatively large  $E$  in Lake Tanganyika is the result of large vapor pressure differences, which would result from high temperatures of air and water.  $H$  is larger in the North American Great lakes because of about 50% greater average wind speeds [Derecki, 1981] and a larger air density, compared with Tanganyika. Low wind speeds and low air density negatively affect  $E$  as well in Lake Tanganyika, but to a much lesser extent than the positive effect of the vapor pressure difference.

[38]  $E$  not only dominates the outputs in the heat budget of Lake Tanganyika, but as a result of the long residence time evaporation also dominates the outputs in the water balance. The amount of water transported by the outflow [Edmond *et al.*, 1993] is much smaller than that lost by evaporation which amounts to more than 90% of the water balance.

[39] Using daily mean data inputs underestimated  $E$  by 4% relative to the results achieved using hourly data ( $p < 0.00001$ , paired *t* test, separately for both basins), in contrast to Quinn [1979], who found no significant differences. The difference in  $E$  caused by the use of daily mean input data is probably the result of nonlinear relations in the algorithm such as the exponential relation between air temperature and vapor pressure.

### 5.3. Effect of Atmospheric Stability

[40] To our knowledge this is the first paper that demonstrates and quantifies the effect of atmospheric stability on latent and sensible fluxes on an annual basis, using data collected on a lake. Earlier papers that determined latent and sensible fluxes in the Laurentian Great Lakes used shorter data sets [Quinn, 1979; Laird and Kristovich, 2002] covering only about 7 months, or used remotely sensed water temperatures in combination with land-based meteorology [Derecki, 1981; Croley, 1989; Lofgren and Zhu, 2000]. The latter is a methodology with many associated problems which are mostly described by Croley [1989], causing large but unknown errors, perhaps contributing to annual mean net surface fluxes that differ substantially from zero [Lofgren and Zhu, 2000]. Our study does not suffer from these problems as the data used in the aerodynamic equations were collected directly on the lake (except humidity which was adjusted for onshore conditions). Only Quinn [1979] quantified the effect of atmospheric stability on latent and sensible fluxes in the Laurentian Great Lakes, but not on an annual basis.

[41] Because of the thermal inertia of water, the surface of lakes warms and cools more slowly than air, and this effect is greater in large and deep lakes. Diurnal and seasonal warming of air is counterbalanced by cooling, which tends to lead to an alternating stable and unstable atmosphere in temperate lakes. A self-regulating heat balance with increased heat loss rates when surface temperatures are high and vice versa is expected to result in surface temperatures that lag behind air temperatures but are on average similar to mean air temperatures [Imberger and Patterson, 1989]. However, it is not the thermal inertia of water alone that results in nonneutral states of the atmosphere above lakes, as at Lake Tanganyika the ABL was nearly permanently (>99% of the time) unstable. While it is often assumed that only at diel time scales the thermal inertia of the water is too great to use constant values of the mass transfer coefficients [Rueda *et al.*, 2007; MacIntyre *et al.*, 2002; Imberger and Patterson, 1989], our results show that on seasonal scales variability in  $C_E$  can be more than 20% (Figure 4b, monthly means). Diel variability in  $C_E$  was similar to daily variability.

[42] The persistent unstable ABL at Lake Tanganyika resulted from high water temperatures that were almost always above those of the air. The water-air temperature difference  $T_o - T$  is often used as an indicator of stability [Derecki, 1981; Schertzer, 1987; Croley, 1989; Rouse *et al.*, 2003], but this overestimates the occurrence of stable conditions. Using

**Table 4.** Effects on  $E$  and Stability for Values of  $\rho_a$ ,  $\nu$ , and  $L_V$  at Air Pressure and Temperature Typical for Temperate Low-Altitude Lakes Such as the North American Great Lakes<sup>a</sup>

Variable	Condition	Value	% Change $E$	% Change $CE$	% Change $(C_E - C_{EN})/C_{EN}$	% Change $(E - E_N)/E_N$
<i>North Basin</i>						
$\rho_a$	Tanganyika mean	1.07				
$\rho_a$	$T = 10^\circ\text{C}$	1.13	+5.2	-0.7	-0.4	-0.5
$\rho_a$	$p = 1013 \text{ mbar}$	1.17	+8.6	-1.2	-0.6	-0.7
$\rho_a$	$T = 10, p = 1013$	1.24	+14.3	-1.9	-1.0	-1.0
$\nu$	Tanganyika mean	0.0000172				
$\nu$	$T = 10^\circ\text{C}$	0.0000156	-1.1	-1.3	-0.7	-0.6
$\nu$	$p = 1013 \text{ mbar}$	0.0000157	-1.0	-1.2	-0.6	-0.6
$\nu$	$T = 10, p = 1013$	0.0000142	-2.1	-2.4	-1.3	-1.2
$L_V$	Tanganyika mean	2,437,887				
$L_V$	$T_o = 10^\circ\text{C}$	2,477,300	+1.6	0.0	+0.0	+0.0
$\rho_a, \nu, L_V$	$T = T_o = 10^\circ\text{C}$		+6.5	-1.3	-0.6	-0.7
$\rho_a, \nu,$	$p = 1013 \text{ mbar}$		+8.6	-1.2	-0.6	-0.7
$\rho_a, \nu, L_V$	$T = T_o = 10, p = 1013$		+15.6	-2.4	-1.1	-1.4
<i>South Basin</i>						
$\rho_a$	Tanganyika mean	1.07				
$\rho_a$	$T = 10^\circ\text{C}$	1.13	+5.2	-0.8	-0.7	-0.4
$\rho_a$	$p = 1013 \text{ mbar}$	1.17	+8.8	-1.4	-1.2	-0.8
$\rho_a$	$T = 10, p = 1013$	1.24	+14.5	-2.2	-1.9	-1.3
$\nu$	Tanganyika mean	0.0000173				
$\nu$	$T = 10^\circ\text{C}$	0.0000156	-1.1	-1.4	-1.3	-0.9
$\nu$	$p = 1013 \text{ mbar}$	0.0000157	-1.0	-1.4	-1.2	-0.9
$\nu$	$T = 10, p = 1013$	0.0000142	-2.1	-2.8	-2.4	-1.8
$L_V$	Tanganyika mean	2,438,035				
$L_V$	$T_o = 10^\circ\text{C}$	2,477,300	+1.6	0.0	0.0	+0.1
$\rho_a, \nu, L_V$	$T = T_o = 10^\circ\text{C}$		+6.4	-1.5	-1.1	-0.8
$\rho_a, \nu,$	$p = 1013 \text{ mbar}$		+8.8	-1.4	-1.2	-0.8
$\rho_a, \nu, L_V$	$T = T_o = 10, p = 1013$		+15.8	-2.8	-2.1	-1.7

<sup>a</sup>The  $\rho_a$  and  $\nu$  are determined by air pressure, air temperature, and humidity, and  $L_V$  is determined by water surface temperature. For the calculations of the effects on  $E$  and stability, only the values of  $\rho_a$ ,  $\nu$ , and  $L_V$  were taken as constant values typical for temperate low-altitude conditions ( $T = 10^\circ\text{C}$ ,  $p = 1013 \text{ mbar}$ ), while air pressure and temperature were maintained at their local tropical values.

this indicator, the atmosphere at Lake Tanganyika would be regarded as being stable 17% of the time (24% in the south basin and 9% of the time in the north basin), instead of 1% in both basins which follows from the sign of  $L$ . However, the atmosphere in the boundary layer is unstable when  $T_V$  decreases with increasing height above the water surface, which occurred more than 99% of the time at Lake Tanganyika. Only when the relative humidity is 100% can  $T_o - T$  be used as an indicator of stability (( $\Delta\theta = T_o - T$  when  $R_H = 100\%$  and  $T_o = T$ ). Including the effect of humidity on the virtual air-surface temperature difference,  $\Delta\theta$ , as an indicator of the stability of the ABL at Lake Tanganyika makes a difference of nearly 2°C (Figure 6).

[43] The difference between  $\Delta\theta$  and  $T_o - T$  increases with decreasing humidity and with increasing  $T_o - T$ . In summary,  $\zeta = 0$  when  $\Delta\theta = 0$ ,  $H = 0$  when  $T_o - T = 0$ ,  $E = 0$  when  $q_s - q_z = 0$ , and  $E = \zeta = H = 0$  only when both  $R_H = 100\%$  and  $T_o - T = 0$  are true. Usually,  $\zeta$  and  $E$  are  $> 0$  when  $H = 0$ , unless  $R_H = 100\%$ , and  $H < 0$  and  $E > 0$  when  $\zeta = 0$ .

[44] While negative  $H$  occurred throughout the summer, from April to July, in each of the Laurentian Great Lakes [Lofgren and Zhu, 2000; Laird and Kristovich, 2002], it occurred less frequently and only in the afternoon in the cool season in Lake Tanganyika (9.3% of the time in the north basin and 23.9% of the time in the south basin). Negative  $E$ , implying a negative vapor pressure difference ( $e_{sat} - e_a < 0$ ) which results in condensation instead of heat loss by evaporation, never occurred at Lake Tanganyika while negative  $e_{sat} - e_a$  and negative  $E$  do occur in summer at the North

American Great Lakes [Derecki, 1981; Schertzer, 1987; Lofgren and Zhu, 2000; Laird and Kristovich, 2002] and at Great Slave Lake [Blanken et al., 2003]. In Lake Tanganyika in the south basin,  $e_{sat} - e_a$  ranged from 9 to 25 mbar (average 15 mbar) and in the north basin from 3 to 22 mbar (average 11 mbar). The lower occurrence of negative  $H$  and absence of negative  $E$  at Lake Tanganyika, compared with the Laurentian Great Lakes, resulted from the persistent higher surface temperatures compared with air temperatures. In tropical Lake Tanganyika, unlike in temperate waters,  $E$  and  $H$  are almost always heat losses (always for  $E$ ) and rarely heat gains to the lake (never for  $E$ ).

[45] In contrast to the almost continuously unstable conditions at Lake Tanganyika, at temperate lakes the atmosphere is stable during spring and summer and unstable during fall and winter [Derecki, 1981; Lofgren and Zhu, 2000; Laird and Kristovich, 2002]. In the higher latitude Great Slave Lake, the atmosphere was stable, on average, 35% of the open water period [Rouse et al., 2003; Blanken et al., 2003]. Derecki [1981] even reported a large negative effect of stability on the annual mean latent heat fluxes in Lake Erie and Lake St. Clair, resulting from stable conditions during summer, while the net effect for Lake Superior was positive because of strongly unstable conditions in winter coinciding with high wind speeds.

[46] Other investigators have also found a usually positive water to air temperature difference in tropical lakes; for example the mean difference  $T_o - T$  over Lake Victoria is +3.1°C [Yin and Nicholson, 1998], more than twice that at

Lake Tanganyika, and the mean  $T_o - T$  is  $2.2^{\circ}\text{C}$  at Lake Toba (905 m above sea level) in Indonesia [Sene *et al.*, 1991]. The continuous positive water to air temperature difference in the tropics probably results from the relative small increase in air temperature during the warm season while the water surface temperature does not cool much in the cool season (Figure 4). In temperate and high-latitude lakes air temperatures in spring are much higher than of the water, and the opposite occurs in the fall. This is not the case in the tropics. In tropical lakes there is no substantial lag in surface temperatures, unlike in temperate waters.

[47] In addition, in low-latitude and high-altitude lakes, a relatively large proportion of the solar radiation is absorbed annually. Toward the equator, the solar angle becomes increasingly perpendicular which reduces albedo. Furthermore, the proportion that reaches the earth surface, of radiation received at the top of the atmosphere, will be relatively large as well in the tropics, because the shorter travel path through the atmosphere and low air density will increase the amount that reaches the earth surface. We propose that, as a result, surface water temperatures are commonly above the air temperatures in tropical lakes on a seasonal time scale. Therefore the ABL is more often unstable over tropical lakes than over temperate lakes and the effect of atmospheric stability on surface heat flux is more consistent in tropical lakes than in temperate lakes.

[48] The generally unstable ABL in tropical lakes, apart from enhancing heat exchange, would be expected to facilitate higher rates of gas exchange [Erickson, 1993] compared with temperate lakes. Enhanced rates of gas fluxes from tropical lakes will affect the global carbon budget because of the much larger  $\text{CO}_2$  disequilibria found on average in tropical lakes compared with temperate lakes [Marotta *et al.*, 2009].

[49] Apart from the latitude effect on atmospheric stability and heat exchange rates, heat absorption by lakes is expected to be enhanced relative to heat absorption by the atmosphere with increasing altitude, because scatter and absorption of solar radiation by air is reduced both by the relatively small travel path through the atmosphere and by lower air density. Because air density is smaller at high elevations sensible heat loss from the lake to the atmosphere is reduced, contributing further to a higher  $T_o - T$  difference. In addition,  $\Delta\theta$  is slightly higher at air pressures lower than at sea level because of the pressure effects on specific humidity. Because of higher absorption and retention of solar energy and higher specific humidity gradients above the lake surface the frequency of unstable conditions is expected to be enhanced at high-altitude lakes. Rueda *et al.* [2007] found mostly unstable conditions during the ice-free season in a mountain lake at 3050 m a.s.l. As a result, heat fluxes are enhanced in high-altitude lakes, as in low-latitude lakes.

[50] The persistent unstable atmosphere in the boundary layer, caused by consistently higher water surface temperatures compared with air temperatures, results in a substantial increase in the average rate of heat loss from Lake Tanganyika. At Tanganyika the atmosphere was unstable >99% of the time and heat transfer coefficients were enhanced by 23% relative to the neutral transfer coefficients. The estimate of the latent heat flux increased 13% as a result of the atmospheric stability. Therefore it increased the estimate of the annually evaporated volume (total  $65 \text{ km}^3$ , or

$1989 \text{ mm yr}^{-1}$ ) at Lake Tanganyika by 13% ( $7.5 \text{ km}^3$ ). The persistent temperature gradient and enhanced loss rates of heat and vapor as a result of an unstable atmospheric boundary layer are likely to be typical for tropical lakes. The hydrological cycle is expected to accelerate with climate change in the East African region [de Wit and Stankiewicz, 2006] and globally [Wentz *et al.*, 2007]. In order to examine the effect of the warming of the surface of Lake Tanganyika and other tropical lakes by climate change [Verburg *et al.*, 2003] on the loss of heat and water vapor to the atmosphere, an understanding of the effect of the atmospheric stability is essential.

[51] **Acknowledgments.** Data were collected by the Research Project for the Management of the Fisheries of Lake Tanganyika, Food and Agriculture Organization, GCP/RAF/271/FIN. We are grateful to many members of the Fisheries Departments of Burundi, Democratic Republic of Congo, Tanzania, and Zambia for assistance with the data collection and maintenance of recorders. The equipment was installed under the supervision of Timo Huttula. Analysis was supported by a Ph.D. research grant under supervision of Bob Hecky, by a Fellowship at the National Center for Ecological Analysis and Synthesis, Santa Barbara (P.V.), and by NIWA. We thank Sally MacIntyre, Matt Hipsey, John Drake, Ian Renfrew, and three anonymous reviewers for comments. This manuscript constitutes CWR reference ED2164JA.

## References

- Amorocho, J., and J. J. De Vries (1980), A new evaluation of the wind stress coefficient over water surfaces, *J. Geophys. Res.*, **85**, 433–442, doi:10.1029/JC085iC01p00433.
- Blanken, P. D., W. R. Rouse, and W. M. Schertzer (2003), Enhancement of evaporation from a large northern lake by the entrainment of warm, dry air, *J. Hydrometeorol.*, **4**, 680–693, doi:10.1175/1525-7541(2003)004<0680:EOEFAL>2.0.CO;2.
- Brutsaert, W. H. (1982), *Evaporation into the Atmosphere: Theory, History, and Applications*, D. Reidel, Dordrecht, Netherlands.
- Businger, J. A., J. C. Wyngaard, Y. Izumi, and E. F. Bradley (1971), Flux-profile relationships in the atmospheric surface layer, *J. Atmos. Sci.*, **28**, 181–189, doi:10.1175/1520-0469(1971)028<0181:FPRITA>2.0.CO;2.
- Croley, T. E., II (1989), Verifiable evaporation modeling on the Laurentian Great Lakes, *Water Resour. Res.*, **25**, 781–792, doi:10.1029/WR025i005p00781.
- de Wit, M., and J. Stankiewicz (2006), Changes in surface water supply across Africa with predicted climate change, *Science*, **311**, 1917–1921, doi:10.1126/science.1119929.
- Derecki, J. A. (1981), Stability effects on Great Lakes evaporation, *J. Great Lakes Res.*, **7**, 357–362, doi:10.1016/S0380-1330(81)72064-1.
- Dyer, A. J. (1967), The turbulent transport of heat and water vapour in an unstable atmosphere, *Q. J. R. Meteorol. Soc.*, **93**, 501–508, doi:10.1002/qj.49709339809.
- Edmond, J. M., R. F. Stallard, H. Craig, V. Craig, R. F. Weiss, and G. W. Coulter (1993), Nutrient chemistry of the water column of Lake Tanganyika, *Limnol. Oceanogr.*, **38**, 725–738.
- Erickson, D. J. (1993), A stability dependent theory for air-sea gas exchange, *J. Geophys. Res.*, **98**, 8471–8488, doi:10.1029/93JC00039.
- Fairall, C. W., E. F. Bradley, D. P. Roger, J. B. Edson, and G. S. Young (1996), Bulk parameterization of air-sea fluxes for Tropical Ocean–Global Atmosphere Coupled-Ocean Atmosphere Response Experiment, *J. Geophys. Res.*, **101**, 3747–3764, doi:10.1029/95JC03205.
- Fairall, C. W., E. F. Bradley, J. E. Hare, A. A. Grachev, and J. B. Edson (2003), Bulk parameterization of air-sea fluxes: Updates and verification for the COARE algorithm, *J. Clim.*, **16**, 571–591, doi:10.1175/1520-0442(2003)016<0571:BPOASF>2.0.CO;2.
- Fisher, H. B., E. J. List, R. C. Y. Koh, J. Imberger, and N. H. Brooks (1979), *Mixing in Inland and Coastal Waters*, Academic, San Diego, Calif.
- Henderson-Sellers, B. (1986), Calculating the surface energy balance for lake and reservoir modeling: A review, *Rev. Geophys.*, **24**, 625–649, doi:10.1029/RG024i003p00625.
- Hicks, B. B. (1975), A procedure for the formulation of bulk transfer coefficients over water, *Boundary Layer Meteorol.*, **8**, 515–524, doi:10.1007/BF02153568.

- Imberger, J., and J. C. Patterson (1989), Physical limnology, *Adv. Appl. Mech.*, 27, 303–475, doi:10.1016/S0065-2156(08)70199-6.
- Katsaros, K. B. (1998), Turbulent flux of water vapor in relation to the wave field and atmospheric stratification, in *Physical Processes in Lakes and Oceans, Coastal Estuarine Stud.*, vol. 54, edited by J. Imberger, pp. 157–172, AGU, Washington, D. C.
- Laird, N. F., and D. Kristovich (2002), Variations of sensible and latent heat fluxes from a Great Lakes buoy and associated synoptic weather patterns, *J. Hydrometeorol.*, 3, 3–12, doi:10.1175/1525-7541(2002)003<0003:VOSALH>2.0.CO;2.
- Laval, B., J. Imberger, B. R. Hodges, and R. Stocker (2003), Modeling circulation in lakes: Spatial and temporal variations, *Limnol. Oceanogr.*, 48, 983–994.
- Lenters, J. D., T. K. Kratz, and C. J. Bowser (2005), Effects of climate variability on lake evaporation: Results from a long-term energy budget study of Sparkling Lake, northern Wisconsin (USA), *J. Hydrol.*, 308, 168–195, doi:10.1016/j.jhydrol.2004.10.028.
- Lofgren, B. M., and Y. Zhu (2000), Surface energy fluxes on the Great Lakes based on satellite-observed surface temperatures 1992–1995, *J. Great Lakes Res.*, 26, 305–314, doi:10.1016/S0380-1330(00)70694-0.
- MacIntyre, S., J. R. Romero, and G. W. Kling (2002), Spatial-temporal variability in surface layer deepening and lateral advection in an embayment of Lake Victoria, *Limnol. Oceanogr.*, 47, 656–671.
- Marotta, H., C. M. Duarte, S. Sobek, and A. Enrich-Prast (2009), Large CO<sub>2</sub> disequilibria in tropical lakes, *Global Biogeochem. Cycles*, 23, GB4022, doi:10.1029/2008GB003434.
- Montgomery, R. B. (1947), Viscosity and thermal conductivity of air and diffusivity of water vapor in air, *J. Meteorol.*, 4, 193–196.
- Quinn, F. H. (1979), An improved aerodynamic evaporation technique for large lakes with application to the International Field Year for the Great Lakes, *Water Resour. Res.*, 15, 935–940, doi:10.1029/WR015i004p00935.
- Renfrew, I. A., G. W. K. Moore, P. S. Guest, and K. Bumke (2002), A comparison of surface layer and surface turbulent flux observations over the Labrador Sea with ECMWF analyses and NCEP reanalyses, *J. Phys. Oceanogr.*, 32, 383–400, doi:10.1175/1520-0485(2002)032<0383:ACOSLA>2.0.CO;2.
- Rouse, W. R., C. M. Oswald, J. Binyamin, P. D. Blanken, W. M. Schertzer, and C. Spence (2003), Interannual and seasonal variability of the surface energy balance and temperature of central Great Slave Lake, *J. Hydrometeorol.*, 4, 720–730, doi:10.1175/1525-7541(2003)004<0720:IASVOT>2.0.CO;2.
- Rueda, F., E. Moreno-Ostos, and L. Cruz-Pizarro (2007), Spatial and temporal scales of transport during the cooling phase of the ice-free period in a small high-mountain lake, *Aquat. Sci.*, 69, 115–128, doi:10.1007/s00027-006-0823-8.
- Schertzer, W. M. (1987), Heat balance and heat storage estimates for Lake Erie, 1967 to 1982, *J. Great Lakes Res.*, 13, 454–467, doi:10.1016/S0380-1330(87)71666-9.
- Schertzer, W. M., W. R. Rouse, and P. D. Blanken (2000), Cross-lake variation of physical limnological and climatological processes of Great Slave Lake, *Phys. Geogr.*, 21, 385–406.
- Schertzer, W. M., W. R. Rouse, P. D. Blanken, and A. E. Walker (2003), Over-lake meteorology and estimated bulk heat exchange of Great Slave Lake in 1998 and 1999, *J. Hydrometeorol.*, 4, 649–659, doi:10.1175/1525-7541(2003)004<0649:OMAEBH>2.0.CO;2.
- Sene, K. J., J. H. C. Gash, and D. D. McNeill (1991), Evaporation from a tropical lake: Comparison of theory with direct measurements, *J. Hydrol.*, 127, 193–217, doi:10.1016/0022-1694(91)90115-X.
- Smith, S. D. (1988), Coefficients for sea surface wind stress, heat flux, and wind profiles as a function of wind speed and temperature, *J. Geophys. Res.*, 93, 15,467–15,472, doi:10.1029/JC093iC12p15467.
- Verburg, P., and R. E. Hecky (2003), Wind patterns, evaporation and related physical variables in Lake Tanganyika, East Africa, *J. Great Lakes Res.*, 29, 48–61, doi:10.1016/S0380-1330(03)70538-3.
- Verburg, P., and R. E. Hecky (2009), The physics of the warming of Lake Tanganyika by climate change, *Limnol. Oceanogr.*, 54, 2418–2430.
- Verburg, P., R. E. Hecky, and H. Kling (2003), Ecological consequences of a century of warming in Lake Tanganyika, *Science*, 301, 505–507, doi:10.1126/science.1084846.
- Wentz, F. J., L. Ricciardulli, K. Hilburn, and C. Mears (2007), How much more rain will global warming bring?, *Science*, 317, 233–235, doi:10.1126/science.1140746.
- Yin, X., and S. E. Nicholson (1998), The water balance of Lake Victoria, *Hydrol. Sci. J.*, 43, 789–811, doi:10.1080/0262669809492173.
- Zeng, X., M. Zhao, and R. E. Dickinson (1998), Intercomparison of bulk aerodynamic algorithms for the computation of sea surface fluxes using TOGA COARE and TAO data, *J. Clim.*, 11, 2628–2644, doi:10.1175/1520-0442(1998)011<2628:IOBAAF>2.0.CO;2.

J. P. Antenucci, Centre for Water Research, University of Western Australia, 35 Stirling Hwy., Crawley, WA 6009, Australia.

P. Verburg, Aquatic Ecology, National Institute of Water and Atmospheric Research, PO Box 11-115, Gate 10 Silverdale Rd, Hamilton 3251, New Zealand. (p.verburg@niwa.co.nz)